View metadata, citation and similar papers at core.ac.uk

brought to you by CORE

東北大学機関リポジトリ
TOUR
Tohoku University Repository

Dynamical Breaking of Charge Neutrality in Intrinsic Josephson Junctions: Common Origin for Microwave Resonant Absorptions and Multiple-Branch Structures in the I-V Characteristics

著者	Machida M., Koyama T., Tachiki M.
journal or publication title	Physical Review Letters
volume	83
number	22
page range	4618-4621
year	1999
URL	http://hdl.handle.net/10097/53236

doi: 10.1103/PhysRevLett.83.4618

Dynamical Breaking of Charge Neutrality in Intrinsic Josephson Junctions: Common Origin for Microwave Resonant Absorptions and Multiple-Branch Structures in the I-V Characteristics

M. Machida
CCSE, Japan Atomic Energy Research Institute, 2-2-54 Nakameguro, Meguro-ku Tokyo 153-0061, Japan

T. Koyama
Institute for Materials Research, Tohoku University, Katahira 2-1-1, Aoba-ku, Sendai 980-8577, Japan

M. Tachiki
National Research Institute for Metals, Sengen 1-2-1, Tsukuba, Ibaraki 305-0047, Japan
(Received 19 March 1999)

We demonstrate that both microwave resonant absorptions and multiple-branch structures in the I-V characteristics observed in intrinsic Josephson junctions are caused by the dynamical breaking of the charge neutrality inside the atomic-scale superconducting layers. The Lagrangian for the time-dependent Lawrence-Doniach model incorporating the charge neutrality breaking effect is proposed. On the basis of the Lagrangian, the longitudinal collective Josephson plasma mode is proved to exist. The branching behaviors in the I-V curves are almost completely reproduced by careful numerical simulations for the model equation derived from the Lagrangian.

PACS numbers: 74.20.De, 74.25.Fy, 74.50.+r, 74.80.Dm

Intrinsic Josephson effects (IJE's) in highly anisotropic high temperature superconductors (HTSC's) [1–3] have attracted growing interests [4,5]. Recent experimental studies have shown two remarkable phenomena for IJE's, i.e., the microwave resonant absorptions [6] and the multiple-branch structures in I-V characteristics along the c axis [1].

In Bi-2212 single crystals, the microwave resonant absorption has been observed for both longitudinal and transverse microwave configurations in cavities. These two configurations yield different dispersion relations [7]. The absorption in the longitudinal configuration has been established to be caused by the excitation of the longitudinal Josephson plasma propagating along the c axis. The existence of such a longitudinal mode indicates the dynamical breaking of the charge neutrality (DBCN) of superconducting layers in the presence of an ac electric field along the c axis. A novel coupling between junctions arising from this effect has been proposed in [8], which may bring about new collective dynamics in IJE.

The I-V curves along the c axis in Bi-2212 form a branch structure with almost equal interbranch spacing, and the number of branches is nearly equal to the number of junctions in the stack [1,9]. It has been widely believed that such a branch structure manifests the independence of junctions; that is, the coupling between junctions is negligible, so that each junction behaves independently [9]. However, such an understanding is irreconcilable with the interpretation for the microwave resonant absorption as mentioned above.

In this paper we claim that both phenomena observed in Bi-2212 have the common origin. A model Lagrangian is proposed which can describe both the longitudinal Josephson plasma and the I-V curves with the multiple-branch structure.

Let us first discuss the essential difference between charge dynamics in the intrinsic Josephson junction systems and that in a conventional superconductor-insulator-superconductor (SIS) array. In Fig. 1 we depicted the physical events accompanying the electron tunneling in both systems. The charge screening length, μ, in the superconducting state is much the same as the Thomas-Fermi length [$\sim O(\text{Å})$] in the normal state and is much shorter than the thickness of superconducting layers in conventional SIS arrays. As a result, the electric field generated at a junction site is completely screened out at the junction site; that is, the charge neutrality inside the superconducting layers is almost strictly maintained. Thus, the longitudinal coupling between

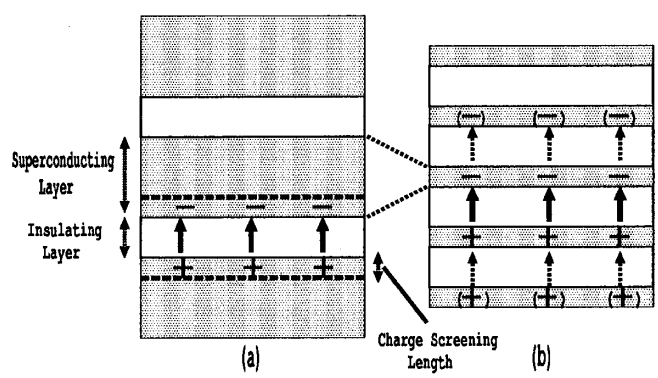

FIG. 1. Schematic views of (a) conventional stacked SIS junction and (b) the intrinsic Josephson junctions. The arrows indicate the direction of the tunneling current and the induced electric field.

 0031-9007/99/83(22)/4618(4)$15.00 © 1999 The American Physical Society

different junction sites is not formed. On the other hand, in HTSC this situation does not hold, because the thickness of superconducting CuO_2 layers ($\sim$3 Å) is comparable with μ. Hence, one may expect that the screening effect is imperfect in a single superconducting layer and then the electric field induced at a junction site penetrates into neighboring junctions. The charge neutrality inside the superconducting layers is thus dynamically broken, and the coupling between junctions appears in intrinsic Josephson-junction systems when the ac Josephson effect is taking place [8,10].

Let us now propose a Lagrangian which describes the DBCN in intrinsic Josephson junctions. Though the pairing mechanism in HTSC has not yet been settled, we may construct a phenomenological model on the basis of the time-dependent Ginzburg-Landau (TDGL) theory, which is basically independent of the detail of the electronic states and the pairing mechanism,

$$L_{\mathrm{LD}} = \sum_{\ell}\left\{\frac{s}{8\pi\mu^2}\left[A_0(z_\ell,t) + \frac{\hbar}{e^*}\,\partial_t\theta_\ell\right]^2 - \frac{\hbar}{e^*}\,j_c(1-\cos P_{\ell+1,\ell}) + \frac{\epsilon D}{8\pi}\,E^2_{\ell+1,\ell}\right\}, \quad (1)$$

where s and D, respectively, are thicknesses of the superconducting and insulating layers, μ is the charge screening length, ϵ is the dielectric constant, $E_{\ell+1,\ell}$ is the electric field ($\perp$ layers) between $(\ell+1)$th and ℓth superconducting layer, $e^* = 2e$, and $P_{\ell+1,\ell}[\equiv \theta_{\ell+1}(t) - \theta_\ell(t) - (e^*/\hbar c)\int_{\ell D}^{(\ell+1)D} dz\, A_z(z,t)]$ is the gauge invariant phase difference. In Eq. (1) the charge density of ℓth superconducting layer, $\rho_\ell(t)$, is expressed as $\rho_\ell(t) = -(1/4\pi\mu^2)[A_0(z_\ell) + (\hbar/e^*)\,\partial_t\theta_\ell]$. This Lagrangian corresponds to a discrete version of the TDGL theory at $T = 0$ K [11,12] for multi-Josephson-junction systems when μ and j_c are taken as $\mu = \sqrt{m^* v_f^2/(12\pi e^{*2}\Delta^2)}$ and $j_c = \hbar e^*\Delta^2/(MD^2)$, where v_f is the Fermi velocity, Δ is the amplitude of the order parameter at $T = 0$ K, and m^* and M are the effective masses parallel and perpendicular to the layers, respectively. The first term in Eq. (1) represents the interaction between the charge density and the scalar potential in superconducting layer. In conventional SIS junction arrays, this term is dropped and the dynamics originating from only the second and third terms in Eq. (1) has so far been intensively studied [12,13]. This is because the coefficient $s/8\pi\mu^2$ is considered to be very large in conventional systems, which indicates that $\mathcal{L}$ has a deep minimum at $\partial_t\theta_\ell = -(e^*/\hbar)A_0(z_\ell)$, i.e., the Josephson relation, and the deviations from this minimum gives high-energy excitations [13]. However, this is not the case in HTSC's, since the thickness, s, of CuO_2 bilayers is comparable with μ. This means that the fluctuations arising from the first term in Eq. (1) cannot be neglected in HTSC's and the charging energy inside the superconducting layers is comparable with that of the ac Josephson effect in Bi-2212. This is the essential point that discriminates the IJE's from the ac Josephson effects in conventional arrays.

Let us now prove that the Lagrangian (1) has the longitudinal plasma mode. To study the response to a longitudinal electric field along the c axis, we derive the dielectric function. In charged systems the Goldstone mode is absorbed into the longitudinal gauge field and the gauge field becomes massive. To describe this situation clearly, we utilize the phason gauge [14], in which the gauge condition is given by $\partial_t A_0(z_\ell) + (v_B^2/c)[(A^z_{\ell+1,\ell} - A^z_{\ell,\ell-1})/D] = 0$, where $A^z_{\ell+1,\ell} \equiv \int_{\ell D}^{(\ell+1)D} dz\, A_z(z)/D$, and $v_B[\equiv \sqrt{(8\pi\mu^2/s)(e^*/2\hbar)j_c}\,D]$ is the phason velocity. Note that the neutral version of Lagrangian (1) without the gauge fields gives the Euler equation for θ_ℓ in the linear approximation as $[-\partial_t^2 + v_B^2(1/D^2)\Delta^{(2)}]\theta_\ell = 0$, with $\Delta^{(2)}\theta_\ell \equiv \theta_{\ell+1} - 2\theta_\ell + \theta_{\ell-1}$. For the gauge transformation, $A^z_{\ell+1,\ell} \to A^z_{\ell+1,\ell} + (\hbar c/e^* D)(\chi_{\ell+1} - \chi_\ell)$, $A_0(z_\ell) \to A_0(z_\ell) - (\hbar/e^*)\partial_t\chi_\ell$, the gauge condition imposes the equation for χ_ℓ, $[-\partial_t^2 + v_B^2(1/D^2)\Delta^{(2)}]\chi_\ell = 0$, which is the same as the Euler equation for θ_ℓ in the neutral case. This result implies that the phason mode can be eliminated by the gauge transformation in this gauge, and the Lagrangian (1) is rewritten as

$$\mathcal{L} = \sum_{\ell}\left\{\frac{s}{8\pi\mu^2}[A_0(z_\ell)]^2 - \frac{\hbar}{e^*}\,j_c\left(1 - \cos\frac{e^* D}{\hbar c}\,A^z_{\ell+1,\ell}\right) + \frac{\epsilon D}{8\pi}\,E^2_{\ell+1,\ell}\right\}. \quad (2)$$

Variation by A_0 in Eq. (2) yields one of the Maxwell equations,

$$E_{\ell+1,\ell} - E_{\ell,\ell-1} = -\frac{s}{\epsilon\mu^2}\,A_0(z_\ell). \quad (3)$$

On the other hand, from $E_{\ell+1,\ell} = -\partial_t A^z_{\ell+1,\ell}/c - [A_0(z_{\ell+1}) - A_0(z_\ell)]/D$, and the gauge condition, it follows that

$$E_{\ell+1,\ell} - E_{\ell,\ell-1} = \frac{D}{v_B^2}\left(\partial_t^2 - \frac{v_B^2}{D^2}\,\Delta^{(2)}\right)A_0(z_\ell). \quad (4)$$

Then, from Eqs. (3) and (4) one finds the dielectric function for the electric field perpendicular to the junctions,

$$\epsilon(\omega,k_z) = 1 - \frac{\omega_{\mathrm{pl}}^2}{\omega^2 - 2\alpha\omega_{\mathrm{pl}}^2[1-\cos k_z(s+D)]}. \quad (5)$$

In deriving Eq. (5) we used the relations, $(s/\epsilon\mu^2)(v_B^2/D) = 4\pi e^* D/\epsilon\hbar = c^2/\epsilon\lambda_c^2 = \omega_{\mathrm{pl}}^2$ and $2v_B^2/D^2 = (8\pi\mu^2/s)(e^*/\hbar)j_c = 2\alpha\omega_{\mathrm{pl}}^2$ with $\alpha = \epsilon\mu^2/sD$. As seen in Eq. (5), the dielectric function has zero points at $\omega(k_z) = \omega_{\mathrm{pl}}\sqrt{1 + 2\alpha[1-\cos k_z(s+D)]}$, and thus, the longitudinal plasma mode propagating along the c axis is found to exist. Note that when the first term in Eq. (1) is dropped, i.e., $\alpha = 0$, this mode has no dispersion.

Let us next examine the dynamics of the gauge-invariant phase difference $P_{\ell+1,\ell}(t)$ in the presence of a transport current I. From the Lagrangian (1) and the modified Josephson relation, $\partial_t P_{\ell+1,\ell}(t) = (e^*/\hbar)V_{\ell+1,\ell}(t) - (4\pi\mu^2 e^*/\hbar)[\rho_{\ell+1}(t) - \rho_\ell(t)]$ [8], we can derive the

equation for $P_{\ell+1,\ell}(t)$ in the presence of a bias current I

$$\frac{1}{\omega_{\rm pl}^2}\,\partial_t^2 P_{\ell+1,\ell}(t) + \sin P_{\ell+1,\ell}(t) + \frac{\beta}{\omega_{\rm pl}}\,\partial_t P_{\ell+1,\ell}(t) = \frac{I}{j_c} - \alpha[\sin P_{\ell+2,\ell+1}(t) - 2\sin P_{\ell+1,\ell}(t) + \sin P_{\ell,\ell-1}(t)], \quad (6)$$

where $\omega_{\rm pl} = c/\sqrt{\epsilon}\,\lambda_c$ and $\beta = 4\pi\sigma\lambda_c/\sqrt{\epsilon}\,c \equiv 1/\sqrt{\beta_c}$ and β_c being the McCumber parameter. In Eq. (6) the dissipative (quasiparticle) current is introduced. Equation (6) was first derived by two of us (T. K. and M. T.) phenomenologically for a stack of the intrinsic Josephson junctions [8], and afterwards Preis *et al.* gave the microscopic basis for this equation [15]. It is noted that the parameter α is the coupling constant between junctions included in the first term in (1); i.e., in the limit of $\alpha \to 0$ Eq. (6) is reduced to the RCSJ model [13]. One also notices that Eq. (6) has a plane wave solution with the dispersion relation of the longitudinal plasma mode [8,10]. From numerical simulations for Eq. (6) we can get the I-V characteristics in intrinsic Josephson-junction systems. In the following we solve Eq. (6) for the system composed of ten identical junctions under the periodic boundary condition. The values of the parameters are chosen as $\alpha = 0.1$ and $\beta = 0.2$, which correspond to the Bi-2212 case [15,16].

Figure 2(I) is a hysteresis loop in the I-V curve. In obtaining this curve, the current I is increased first above the critical current j_c and then decreased to zero along the arrows in Fig. 2(I). In the current increasing process, we find a jump at j_c, where all junctions synchronously switch into the same resistive states. In Fig. 2(II), the time developments of the normalized Josephson currents $\sin P_{\ell+1,\ell}$ at point B are plotted for all the junction sites. The figure shows that all the junctions synchronously whirl. Further current decrease causes several steplike structures as seen in Fig. 2(I). Figures 2(III) and 2(IV) show the time developments of $\sin P_{\ell+1,\ell}$ of all junction sites at points C and D, respectively. Some junctions are in the resistive state, in which $\sin P_{\ell+1,\ell}$ periodically varies from -1 to 1, while the others are in the superconducting state with tiny oscillations. By monitoring the time evolution of $\sin P_{\ell+1,\ell}$ around C and D one may see that the number of resistive junctions decreases as the current decreases through the steps. Such behavior is never observed in the absence of the coupling ($\alpha = 0$), in which all the resistive junctions switch into the superconducting state at a constant current value.

Let us now study the region around the points C and D in more detail. Figure 3(a) shows the I-V curve enlarged in the region around C and D. In this region, we get different I-V curves when a decreasing interval δI is changed. In Fig. 3(a), two cases with different δI are plotted. These behaviors imply that several bifurcation points are distributed in this narrow region of the parameter I. Hence, we performed the calculations many times, changing δI, to get all the branches (trajectories). When the current is reincreased from points on the branches along the arrows as seen in Fig. 3(a), the multiple-branch structure appears as Fig. 3(b). The obtained I-V curves are composed of equidistant branches and the number of

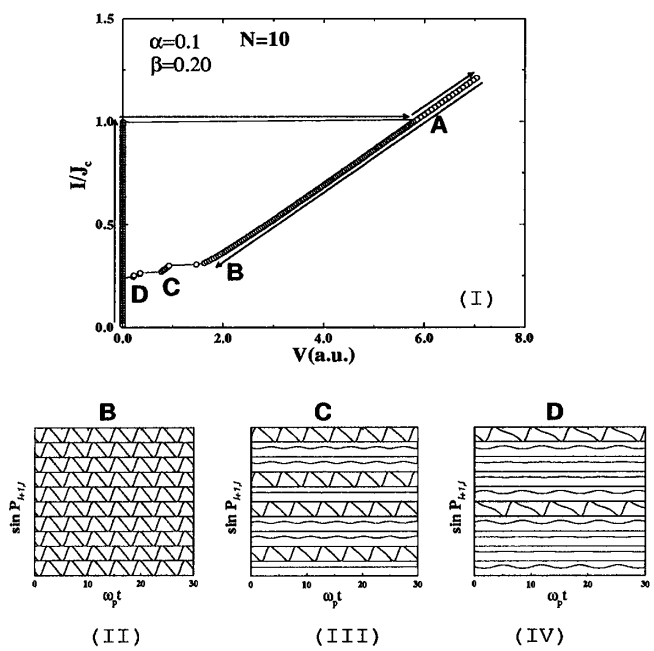

FIG. 2. (I) The I-V hysteresis curve. The current is increased and decreased along the arrows. The time development of $\sin P_{\ell+1,\ell}$ on the junctions from $\ell = 0$ to 9 at points (II) B, (III) C, and (IV) D.

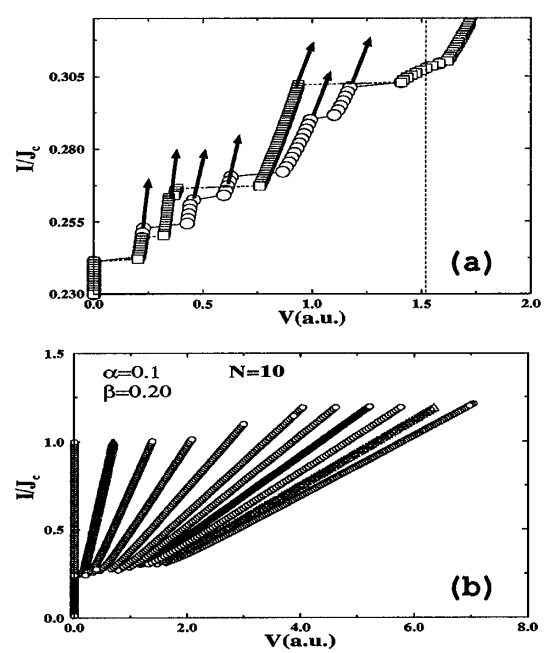

FIG. 3. (a) The enlarged view of the transition region in the I-V curves. The points indicated by circles and squares are those on two different I-V curves obtained for different current intervals. (b) The multiple-branch structure obtained by the current reincreasing process.

branches (= 10) is equal to the number of junctions in this system. In this simulation we introduced the Nyquist noise to get the first and ninth branches. These results indicate that all the resistive branches correspond to the stable trajectories of Eq. (6); that is, Eq. (6) can reproduce the multiple-branch structure without any inhomogeneities of the junction parameters. In real experiments to get the multiple branches one has to repeat the current increasing and decreasing processes many times. These experimental processes are equivalent to the processes in our simulations to get all the bifurcations as seen in Fig. 3(a). Also, we mention that if a free boundary condition is employed, in which peculiarities of the top and bottom junctions are considered, all the branches can be obtained without noise.

Finally we discuss why Eq. (6) can give the multiple-branch structure. To answer this we have to clarify the two points, that is, why the steplike transitions appear in the current decreasing process as seen in Fig. 3(a) and why the branches are stable in the current reincreasing process. In this paper we concentrate on the first point, since Takeno *et al.* have already touched the latter question in the context of the stability of localized whirling (rotating) motions in coupled rotator models [17] and have shown that the bounded character of the trigonometric functions in the coupling terms is essential for the stability of the localized rotating motions. As shown before, the steplike jumps seen in Fig. 3(a) result from the transitions of the resistive junctions into the superconducting state. This fact implies that each junction can switch to the superconducting state at a different current value from one another, though all the junctions are equivalent. Such a behavior reminds us about a stack of independent junctions with different junction parameters. Note that the total driving force (current) on the right-hand side of Eq. (6) is composed of two components, i.e., the external current I/j_c and the Josephson currents at neighboring junction sites, $\tilde{I}_\ell = -\alpha[\sin P_{\ell+2,\ell}(t) + \sin P_{\ell,\ell-1}(t)]$, when the on-site term, $\sin P_{\ell+1,\ell}(t)$, is transposed to the left-hand side of Eq. (6). This fact indicates that the total driving force acting on each junction depends on the dynamical state of neighboring junctions. Let us now investigate the case in which both of the nearest neighbor ($\ell \pm 1$th) junctions are in the superconducting or in the resistive state, supposing that the ℓth junction is in the resistive state. In the former case $\tilde{I}_\ell$ is very small, since the Josephson current on the neighboring junctions shows tiny oscillations around stable points. As a result, the total driving current is nearly equal to the external current I/j_c. On the other hand, in the latter case, the minimum of the instantaneous driving current is given by $I/j_c - 2\alpha$; that is, we have a moment at which the total driving current is sufficiently smaller than I/j_c in this case. This observation indicates that the transition to the superconducting state is more likely to occur in the latter configuration than in the former one. Hence, the present system has more than one switching current and the transition points are distributed in some range of the parameter I. From these considerations one may conclude that the switching between branches in the I-V characteristics is caused by the coupling between junctions due to the imperfect charge screening of the CuO_2 layers along the c axis, i.e., the dynamical charge neutrality breakdown.

In conclusion, we have shown that the charge neutrality inside the superconducting layers in intrinsic Josephson junction is dynamically broken, and the microwave resonant absorption and the multiple branch structure in the I-V curves are caused by this effect. The effective Lagrangian which can describe these phenomena has been proposed.

M. M. thanks C. Helm and H. Matsumoto for illuminating discussions, and also thanks CREST of JST and staff members in JAERI for their support.

[1] R. Kleiner, F. Steinmeyer, G. Kunkel, and P. Müller, Phys. Rev. Lett. **68**, 2394 (1992).
[2] G. Oya, N. Aoyama, A. Irie, S. Kishida, and H. Tokutaka, Jpn. J. Appl. Phys. **31**, L829 (1992).
[3] K. Tamasaku, Y. Nakamura, and S. Uchida, Phys. Rev. Lett. **69**, 1455 (1992).
[4] M. Tachiki, T. Koyama, and S. Takahashi, Phys. Rev. B **50**, 7065 (1994).
[5] L. N. Bulaevskii, M. P. Maley, and M. Tachiki, Phys. Rev. Lett. **74**, 801 (1995).
[6] Y. Matsuda *et al.*, Phys. Rev. Lett. **75**, 4512 (1995).
[7] I. Kakeya *et al.*, Phys. Rev. B **57**, 3108 (1998).
[8] T. Koyama and M. Tachiki, Phys. Rev. B **54**, 16 183 (1996).
[9] K. Schlenga *et al.*, Phys. Rev. B **57**, 14 518 (1998), and references therein.
[10] M. Machida, T. Koyama, and M. Tachiki, Physica (Amsterdam) **300C**, 55 (1998).
[11] M. J. Stephen and H. Suhl, Phys. Rev. **13**, 797 (1964); E. Abraham and T. Tsuneto, Phys. Rev. **152**, 416 (1966).
[12] E. Šimánek, *Inhomogeneous Superconductors* (Oxford University Press, New York, 1994), and references therein.
[13] V. Ambegaokar, U. Eckern, and G. Schon, Phys. Rev. Lett. **48**, 1745 (1982); U. Eckern, G. Schon, and V. Ambegaokar, Phys. Rev. B **30**, 6419 (1984).
[14] H. Matsumoto and H. Umezawa, Fortschr. Phys. **24**, 357 (1976).
[15] Ch. Preis, Ch. Helm, J. Keller, A. Sergeev, and R. Kleiner, in *Superconducting Superlattices II*, SPIE Conference Proceedings (SPIE, Bellingham, WA, 1998), p. 236.
[16] In our previous paper [10] we chose $\alpha = 2.27$ for the Bi-2212 case. This value is too large for the system; see also [15].
[17] S. Takeno and M. Peyard, Physica (Amsterdam) **92D**, 140 (1996); see also Z. Zheng, B. Hu, and G. Hu, Phys. Rev. E **57**, 1139 (1984).